Sonderdruck

EDV in Medizin und Biologie

EDP in Medicine and Biology

Band 17
Heft 1/2/1986

ISSN 0300-8282

Gustav Fischer Verlag Stuttgart · Verlag Eugen Ulmer Stuttgart

EDV in Medizin und Biologie **17** (1/2), 20–27, ISSN 0300-8282

On the use of growth and decay functions for modelling stem profiles

C. Brink and K. von Gadow

Summary

One of the most useful tools for modelling the effects of environmental and stand treatment factors on stem form is a simple taper equation. This article presents four new taper functions for modelling stem profiles. These are not derived de novo, but from known growth and decay functions. The paper demonstrates that it is possible to modify any growth or decay function with certain structural properties to serve as a taper function.

Zusammenfassung

Wenn man die Auswirkungen von Umgebungs- und Behandlungsfaktoren auf die Form von Baumschäften untersuchen will, empfiehlt sich die Anwendung einer flexiblen Schaftgleichung mit begrenzter Parameterzahl. Eine Spline Approximation ist für diesen Zweck unbrauchbar. In diesem Beitrag werden vier neue Schaftgleichungen vorgestellt. Die Gleichungen werden nicht de novo, sondern von bekannten Wachstums- und Zerfallfunktionen abgeleitet. Es wird gezeigt, daß es möglich ist, jede Wachstums- oder Zerfallfunktion mit bestimmten strukturellen Eigenschaften so zu modifizieren, daß sie als Schaftgleichung verwendet werden kann.

1. Introduction

Foresters need to be able to estimate the stem form of trees and how it is affected by environment and stand treatment. One method of modelling the stem form of a tree involves the use of a taper, or stem profile equation which expresses radius r as a function of height h.

One of the first attempts to model the stem profile is BEHRE's (1923) hyperbola (see PRODAN (1965), p. 62):

$$q = \frac{x}{a+bx} \tag{1.1}$$

where

x = relative tree height;
q = relative tree diameter;
a,b = parameters to be estimated.

More recent attempts to model stem profiles include ORMEROD's (1973) equation

$$d = D\left[\frac{H-h}{H-k}\right]^p \qquad (1.2)$$

where

d = diameter (cm) at tree height h (m);
D = diameter (cm) at breast height k (m);
H = total tree height (m) with $0 < h < H$;
p = parameter to be estimated ($p > 0$);
k = 1.35 (breast height).

Because of its simplicity, ORMEROD's equation appears to be rather popular (REED and BYRNE (1985)). Other noteworthy models of stem taper are, for example the dual equation system proposed by DEMAERSCHALK and KOZAK (1977), a system using 4th degree polynomials (MADSEN (1982)) and a recent approach involving the Chapman-Richards function (BINGING (1984)).

We find that a taper equation is a useful tool for modelling stem form. On the one hand, it is flexible enough to provide good estimate of radius at different heights, on the other hand it is simple enough to allow parameter smoothing, consequently permitting better insight into the relationship between stem form, tree dimensions and stand treatment.

In this article we present four new taper functions. Whereas the general tendency seems to be to derive such functions *de novo*, we take the methodologically simpler approach of modifying known growth and decay functions to serve as taper functions. The motivation for this approach is best explained by reference to an idealized stem form, as pictured in Fig. 1.1, which we call the *target shape*. In Fig. 1.1, h indicates tree height and r tree radius; b is breast height (1.35 m) and r_b is radius at breast height; H is the total tree height and r_0 the radius at the base of the stem (the initial radius). So if we view r as a function of h we have $r(0) = r_0$, $r(b) = r_b$ and $r(H) = 0$. The target shape is monotone decreasing, with the curvature at first anti-clockwise, then zero at a point of inflection, and then clockwise. In Fig. 1.1 the point of inflection occurs at the point (I,i), where height is I and the corresponding radius r(I) is i. We call that part of the target shape where $0 \leq h \leq I$ the *initial part*, and the part where $I \leq h \leq H$ the *terminal part* of the target shape. The point to note is that *change of curvature*

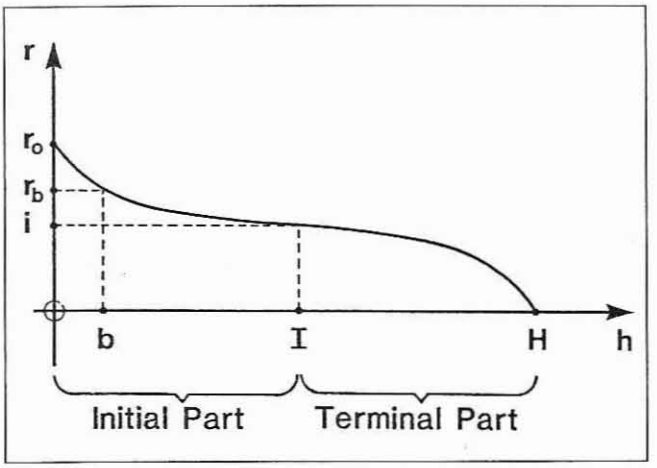

Fig. 1.1. Idealized stem profile or »target shape«.

takes place (mathematically: the second derivative of r changes sign). Whenever this happens, the function in question exhibits an S-shape around the point of inflection, no matter what the orientation of the function is with regard to the axes. In Figure 1.1 the S-shape is best seen by rotating the figure anti-clockwise through ninety degrees. It is well known that an S-shape may be modelled by a variety of functions, usually viewed as growth functions. In principle, then, any one of these functions can also be used as a taper function modelling stem forms. In practice, of course, the choice of such functions depends on considerations such as possible physical interpretation of parameters and techniques available for parameter estimation.

In this article we modify in §3 the logistic function and in §4 the Weibull growth function for use as taper functions. Beforehand, in §2, we obtain two taper functions by modifying a decay function.

We test each of the four taper functions presented here against ten *Eucalyptus cloeziana* trees, the measurements of which are listed in Table 1.1. The results are listed in tables, one for each model. In line with the minimum data usually available for a particular tree, we list in these tables *diameter at breast height over bark* (DBH O-B) and *total height* (H in Figure 1.1). However, for the testing of the models we do not

Table 1.1. Heights (h) and radii (r, under bark) of 10 *Eucalyptus cloeziana* trees.

Tree number																			
116		121		127		128		138		139		142		147		149		152	
h m	r cm	h m	r cm	h m	r cm	h m	r cm	h m	r cm	h m	r cm	h m	r cm	h m	r cm	h m	r cm	h m	r cm
0	9.78	0	11.43	0	8.38	0	7.75	0	8.51	0	7.37	0	9.52	0	6.86	0	9.91	0	9.78
0.6	8.89	0.6	10.29	0.6	7.37	0.6	6.73	0.6	7.62	0.6	6.73	0.6	8.89	0.6	6.35	0.6	8.76	0.6	9.02
1.2	8.38	1.2	9.40	1.2	6.86	1.2	6.10	1.2	6.60	1.2	6.10	1.2	8.13	1.2	5.46	1.2	8.26	1.2	8.51
1.35	8.36	1.35	9.34	1.35	6.81	1.35	6.02	1.35	6.14	1.35	6.06	1.35	7.92	1.35	5.26	1.35	8.21	1.35	8.45
2.4	8.00	2.4	8.89	2.4	6.73	2.4	5.97	2.4	5.59	2.4	5.84	2.4	7.62	2.4	5.08	2.4	7.75	2.4	8.13
4.9	7.37	4.9	7.87	4.9	6.22	4.9	5.08	4.9	5.08	4.9	5.08	4.9	6.86	4.9	4.83	4.9	7.37	4.9	7.24
7.3	6.60	7.3	7.24	7.3	5.59	7.3	4.32	7.3	4.32	7.3	4.57	7.3	6.22	7.3	3.94	7.3	6.35	7.3	6.60
9.8	5.97	9.8	6.35	9.8	4.95	9.8	3.56	9.8	3.68	9.8	3.81	9.8	5.46	9.8	3.18	9.8	5.72	9.8	5.97
12.2	5.08	12.2	5.59	12.2	4.19	12.2	2.92	12.2	2.92	12.2	3.05	12.2	4.57	12.2	1.52	12.2	4.95	12.2	5.08
14.6	4.32	14.6	4.44	14.6	3.30	15.2	1.40	14.9	1.40	15.2	1.52	14.6	3.81	13.1	0	14.6	3.94	14.6	4.19
17.1	3.30	17.1	3.43	17.1	1.65	18.6	0	18.0	0	18.3	0	17.1	1.90			17.7	1.90	17.1	2.79
20.1	1.65	19.2	1.65	19.8	0							19.8	0			21.0	0	18.9	1.40
21.6	0	21.3	0															20.7	0

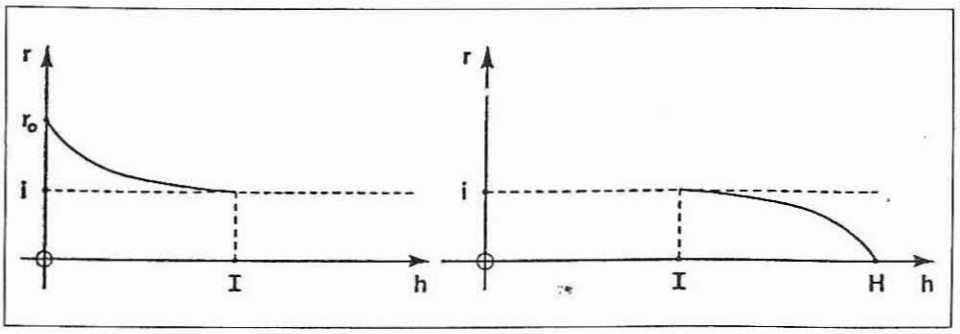

Fig. 2.1. Initial part and termina part of target shape viewed separate ly. Both may be regarded as decay functions.

use DBH O-B but r_b – *radius at breast height under bark.* In fact, all the radii listed in Table 1.1 are taken under bark. Moreover, although nothing in the mathematical development depends on this, we try where possible to arrange matters in such a way that the taper function passes precisely through the points (b, r_b) and (H,0).

2. Application of the classic decay function

We start out by noting that if we view the initial part and the terminal part of the target shape separately, as in Figure 2.1, both of them may be considered as decay functions. Standard models of decay are therefore applicable in both cases. We choose to use what we call the *classic decay function,* namely the solution of the differential equation

$$\frac{dy}{dx} = k\,(y - B), \tag{2.1}$$

which says that the rate of change of y as a function of x is directly proportional to the difference between y and some constant (upper or lower) limit B. (Example: Newton's law of cooling says that the rate of cooling of a warm body is directly proportional to the difference between its own temperature and the (constant and lower) temperature of its environment.)

Using (2.1), we model the initial shape by a function α of h, using i as a lower limit and r_0 as an initial value. So (2.1) becomes

$$\frac{d\alpha}{dh} = -p\,(\alpha - i) \quad (p > 0) \tag{2.2}$$

and standard methods yield the solution

$$\alpha\,(h) = i + (r_o - i)\,e^{-ph}. \tag{2.3}$$

Similarly we model the terminal shape by a function β of h using i as an upper limit and H as an initial *(sic!)* value. In this case the differential equation

$$\frac{d\beta}{dh} = -q\,(i - \beta) \quad (q > 0) \tag{2.4}$$

yields the solution

$$\beta\,(h) = i - ie^{q(h-H)}. \tag{2.5}$$

The models α and β are illustrated in Figure 2.2. Note that neither passes precisely through the point of inflection; this is of course a consequence of using i as a limiting value.

Note further that in each case, the proportionality constant is easily determined from one further data point. Thus if (X, x) is any data point in the initial part, and (Y, y) any data point in the terminal part, then (2.3) and (2.5) respectively show that

$$p = \frac{1}{X} \ln\left(\frac{r_0 - i}{x - i}\right) \tag{2.6}$$

and

$$q = \frac{1}{(Y - H)} \ln\left(\frac{i - y}{i}\right) \tag{2.7}$$

which can be used as initial values when estimating the parameters.

A first model of the target shape may now be constructed by the simple expedient of subtracting from α the difference between i and β. Call the resulting function r_1, then

$$r_1(h) = i + (r_0 - i)e^{-pH} - ie^{q(h-H)}. \tag{2.8}$$

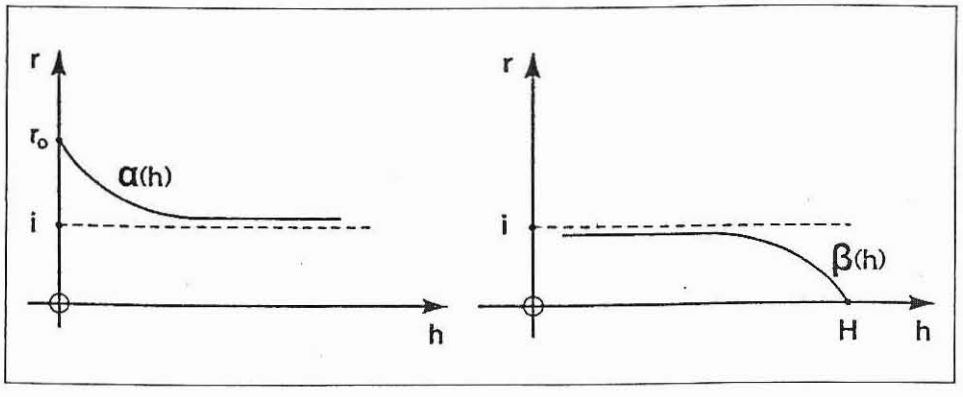

Fig. 2.2. Models for the initial pai and terminal part, respectively, c the target shape. Both are obtaine from the classic decay function.

Thus r_1 lies slightly below α in the initial part and slightly above β in the terminal part. In this function r_0 and H are empirically given, and the parameters i, q and p are calculated using standard nonlinear regression methods. The function is therefore fully determined by the data, is theoretically quite simple, and, as is shown in Table 2.1, is fairly accurate.

A second model may be constructed from the classic decay function by using in (2.2) a variable lower limit in place of the constant lower limit i; the idea being to bend down the graph of α in Figure 2.2 so as to cross the horizontal axis and thus model also the terminal shape. And in fact such a variable lower limit is at hand – we simply use β. Rechristening α as r_2, we get in this way the differential equation

$$\frac{dr_2}{dh} = -p\,(r_2 - \beta),$$

which may be rewritten as

$$\frac{dr_2}{dh} + pr_2 = p\beta \quad (p > 0) \tag{2.9}$$

to show that it is first-order linear. Applying the standard method of solution for this type of differential equation, and using the initial value r_0, we obtain

$$r_2(h) = i - \frac{pi}{p+q}\, e^{q(h-H)} + \left[r_0 - i + \frac{pi}{p+q}\, e^{-qH}\right] e^{-ph} \tag{2.10}$$

this being our second model. Again r_0 and H are given and the parameters are determined as in the first model. On the assumption that the initial part of r_2 closely follows the shape of α, and the terminal part the shape of β, the initial values for p and q found in (2.6) and (2.7) may be used as initial values for parameter estimation of r_2 as well.

To compare the two models r_1 and r_2, rewrite r_2 as

$$r_2(h) = i + (r_0 - i)\, e^{-ph} - \frac{pi}{p+q}\left[e^{q(h-H)} - e^{-ph-qH}\right], \tag{2.11}$$

then it is clear that, like r_1, r_2 is obtained by subtracting an auxiliary function from the classic decay function α of (2.3). Given that p, q, h and H are all positive, we observe that

$$\frac{pi}{p+q} < i$$

and

$$e^{q(h-H)} - e^{-ph-qH} < e^{q(h-H)}.$$

Consequently, $\frac{pi}{p+q}\left[e^{q(h-H)} - e^{-ph-pH}\right] < ie^{q(h-H)}$

and so, these being precisely the auxiliary functions subtracted from α in (2.11) and (2.8) to obtain r_2 and r_1 respectively, we conclude that r_2 lies between α and r_1. If, therefore, we take α and β as describing precisely the initial shape and the terminal shape respectively, then of r_1 and r_2, the latter will be the better model in the initial part, the former in the terminal part. (Since $\beta < r_1 < \alpha$, with $\alpha - r_1$ small in the initial part, and $r_1 - \beta$ small in the terminal part). But of course α and β are just models themselves, and so the relative accuracy of r_1 and r_2 can in practice not be settled in this way.

Table 2.1. Fitting equation (2.8) to the 10 *Eucalyptus cloeziana* trees in Table 1.1.

Tree No.	DBH O.B	Total Height	i	p	q	Error Mean Square
116	18.0	21.64	4.856	0.0720	0.1010	0.068
121	20.6	21.34	7.864	0.3109	0.1317	0.069
127	15.5	19.81	6.658	0.4059	0.1330	0.070
128	13.2	18.59	4.787	0.2376	0.1297	0.081
138	13.7	17.98	4.910	0.3976	0.1558	0.092
139	13.2	18.29	4.837	0.2292	0.1503	0.047
142	17.5	19.81	6.542	0.2507	0.1540	0.049
147	11.9	13.10	4.442	0.2561	0.1620	0.107
149	18.0	21.03	7.216	0.2446	0.1208	0.113
152	18.0	20.73	6.942	0.2170	0.1438	0.029

Table 2.2 Fitting equation (2.14) to the 10 *Eucalyptus cloeziana* trees listed in Table 1.1.

Tree No	DHB O.B.	Total Height	i	p	q	Error Mean Square
116	18.0	21.64	10.21	0.6894	0.0650	0.027
121	20.6	21.34	13.77	1.4654	0.0518	0.056
127	15.5	19.81	9.00	3.1447	0.0773	0.023
128	13.2	18.59	13.72	2.4542	0.0319	0.050
138	13.7	17.98	9.16	1.1155	0.0541	0.135
139	13.2	18.29	10.09	2.2126	0.0520	0.028
142	17.5	19.81	10.77	1.7110	0.0670	0.072
147	11.9	13.10	7.64	1.7711	0.0705	0.135
149	18.0	21.03	12.72	2.8174	0.0514	0.039
152	18.0	20.73	12.11	2.1786	0.0595	0.042

In some cases it may be desired of a function modelling stem profiles to pass *precisely* through selected points – e.g. radius at breast height. For the classic decay function α this is easily effected by using $r(b) = r_b$ as an initial value in (2.2) (instead of $r(0) = r_0$) to obtain

$$\alpha(h) = i + (r_b - i)\, e^{p(b-h)}. \tag{2.12}$$

For our first model r_1, this easy option is not available, since r_1 does not appear here as the solution of a differential equation. But r_2 does, so we may use $r(b) = r_b$ as an initial value in (2.9) to obtain

$$r_2(h) = i - \frac{pi}{p+q}\, e^{q(h-H)} + \left[r_b - i + \frac{pi}{p+q}\, e^{q(b-H)}\right] e^{p(b-h)} \tag{2.13}$$

instead of (2.10). Again, for purpose of comparison this may be rewritten as

$$r_2(h) = i + (r_b - i)\, e^{p(b-h)} - \frac{pi}{p+q}\left[e^{q(h-H)} - e^{q(b-H)+p(b-h)}\right] \tag{2.14}$$

where r_2 then again appears as the result of subtracting an auxiliary function from the classic decay function – (2.12) in this case. For comparison Table 2.2 does for r_2 what Table 2.1 did for r_1.

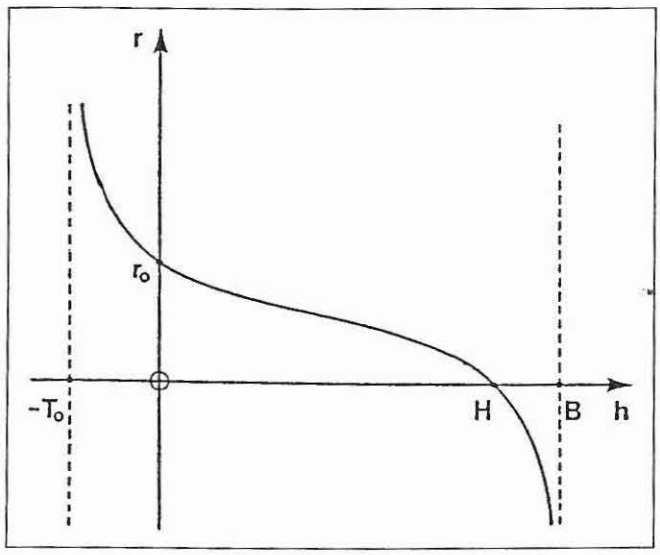

Fig. 3.1. The target shape extended into the second and fourth quadrants. It is assumed to be delimited by two vertical asymptotes.

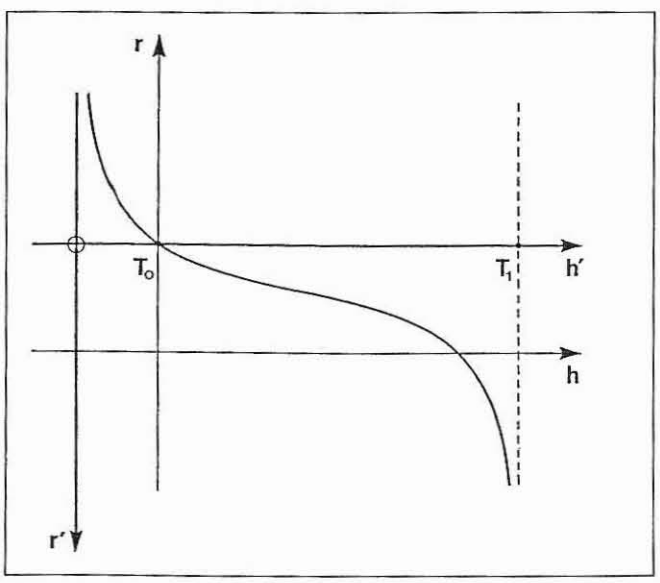

Fig. 3.2. The same graph as in Figure 3.1, but showing the new axes h' and r'.

Table 3.1. Fitting equation (3.7) to the 10 *Eucalyptus cloeziana* trees listed in Table 1.1.

Tree No	DBH O.B.	Total Height	k	T_0	B	Error Mean Square
116	18.0	21.64	0.0086	11.779	27.54	0.118
121	20.6	21.34	0.0283	0.812	21.34	0.144
127	15.5	19.81	0.0090	20.992	22.27	0.186
128	13.2	18.59	0.0468	0.424	19.31	0.149
138	13.7	17.98	0.0518	0.174	17.98	0.169
139	13.2	18.29	0.0434	1.021	18.99	0.103
142	17.5	19.81	0.0341	1.046	20.30	0.199
147	11.9	13.10	0.0677	0.288	16.81	0.246
149	18.0	21.03	0.0157	5.962	22.86	0.228
152	18.0	20.73	0.0145	7.452	22.39	0.103

3. Application of the logistic function

Recall that both models of §1 were constructed by using a horizontal asymptote. This asymptote (the line r = i) was a purely theoretical entity which played no part in the eventual models, except insofar as it influenced the derivation of the equations constituting these models. In the same spirit we now construct a third model by using two vertical asymptotes. We assume, namely, that if the target shape extended also into the second and fourth quadrants it would naturally assume a shape as in Figure 3.1, with the lines $h = -T_0$ and $h = B$ acting as vertical asymptotes. In order to model this extended target shape, we first effect a translation and re-orientation of axes by the equations

$$h' = h + T_0$$
$$r' = r_0 - r, \tag{3.1}$$

so that the target shape appears with respect to the new axes as in Figure 3.2; with $T_1 = B + T_0$. We then assume that

(a) the rate of change of r' is inversely proportional to h'; and
(b) the rate of change of r' is inversely proportional to $T_1 - h'$.

Each of these assumptions is modelled by a differential equation. Combining these in the standard way, and presenting the constant of proportionality as a reciprocal, we get the single differential equation

$$\frac{dr'}{dh'} = \frac{1}{kh'(T_1 - h')} \quad (k > 0). \tag{3.2}$$

Using the initial value $h'(0) = T_0$ we obtain by standard methods the solution

$$r' = \frac{1}{kT_1} \ln \left[\frac{h'B}{T_0 (T_1 - h')}\right],$$

which, translated back to the original axes, becomes

$$r(h) = r_0 - \frac{1}{kT_1} \ln \left[\frac{(h + T_0) B}{(B - h) T_0}\right]. \tag{3.3}$$

The constant of proportionality is easily determined from one further data point. E.g. from r(H) = 0 we obtain

$$k = \frac{1}{r_0 T_1} \ln \left[\frac{(H + T_0) B}{(B - H) T_0}\right] \tag{3.4}$$

which can be used as initial value in the parameter estimation procedure.

As in the first model r_0 and H are empirically given. We do not at this stage attempt to offer an interpretation of the parameters T_0 and B, except to mention that B may be related to the concept of maximum possible height under optimum conditions.

The perceptive reader may have noticed that the present model is in fact a variation of the logistic model of a growth curve. This fact may be illustrated by rotating Figure 3.2 anticlockwise through ninety degrees, in which case h' appears as a function of r' in the familiar S-shape of the logistic function. More precisely, the relationship is exhibited by the fact that

$$\frac{dh'}{dr'} = kh' (T_1 - h'), (k > 0) \tag{3.5}$$

which follows directly from (3.2) by taking reciprocals, and is of course the differential equation of which the logistic curve is a general solution. In fact, solving (3.5) with initial valual h' (0) = T_0 yields the logistic function

$$h' = \frac{T_0 T_1}{(T_1 - T_0)\, e^{-T_1 k r'} + T_0}. \tag{3.6}$$

And the relationship between this function and our model (3.3) of a taper function is that each may be obtained from the other by using the translation equations (3.1).

Should it be required that the function (3.3) pass precisely through a selected point, this may easily be effected by using that point as an initial value in place of $h'(0) = T_0$. For example, if (3.3) is required to pass through (b,r_b), we obtain from (3.1) the information that $h'(r_0 - r_b) = b + T_0$, and using this as an initial value in solving (3.5) we get

$$r(h) = r_b - \frac{1}{kT_1} \ln \left[\frac{(h + T_0)(B - b)}{(B - h)(T_0 + b)}\right]. \tag{3.7}$$

Corresponding to (3.4) we obtain in this case

$$k = \frac{1}{r_b T_1} \ln \left[\frac{(H + T_0)(B - b)}{(B - H)(T_0 + b)}\right]. \tag{3.8}$$

An assessment of this model appears in Table 3.1.

4. Application of the Weibull function

The mathematical gymnastics of 3 (Application of the logistic function) notwithstanding, the model constructed there may be regarded as being obtained from the logistic function by a translation and re-orientation of axes. In effect, then, we obtained a taper function by the simple expedient of rotating a growth function. This is a general method which may be applied to any growth function, and with that a whole class of taper functions became available. For example, the known growth functions of WEIBULL, MITSCHERLICH, VON BERTALANFFY and GOMPERTZ all yield corresponding taper functions. In each case, the taper function obtained in this way, inherits all the structural characteristics of the original growth function.

Thus, for example, the taper function of 3 is symmetric around its point of inflection, since this is a property of the logistic function. This taper function is therefore not a satisfactory model of stem forms in which the curvature of the initial part differs from that of the terminal part. For such stem forms we obtain in this section a taper function from the Weibull growth function.

We use here the Weibull growth function as characterized by YANG, KOZAK and SMITH (1978) and illustrated in Figure 4.1:

$$h' = B - Be^{-(r'/\alpha)^{\beta}}, \tag{4.1}$$

where h' is a function of r', B is an upper limit for h', $\alpha > 0$ is a scale parameter and $\beta > 0$ is a shape parameter.

Adapting now to our present purposes the equations (3.1) we effect a clockwise rotation through ninety degrees by

$$\begin{aligned} h' &= h \\ r' &= r_0 - r, \end{aligned} \tag{4.2}$$

so that the curve of Figure 4.1 re-appears as in Figure 4.2, where we restrict it to the first quadrant. Substituting (4.2) into (4.1) leads to

$$\beta \ln (r_0 - r) - \beta \ln \alpha = \ln \left[\ln \left(\frac{B}{B - h}\right)\right], \tag{4.3}$$

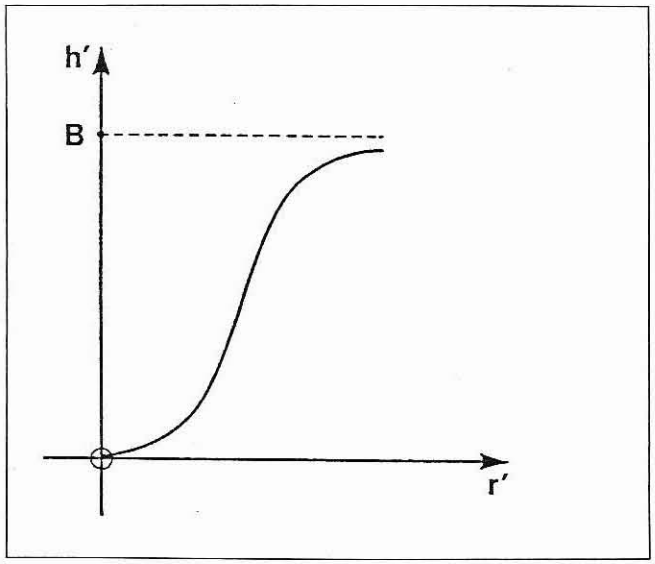

Fig. 4.1. Characteristic S-shaped growth function, here assumed to be modelled by the Weibull function (4.1).

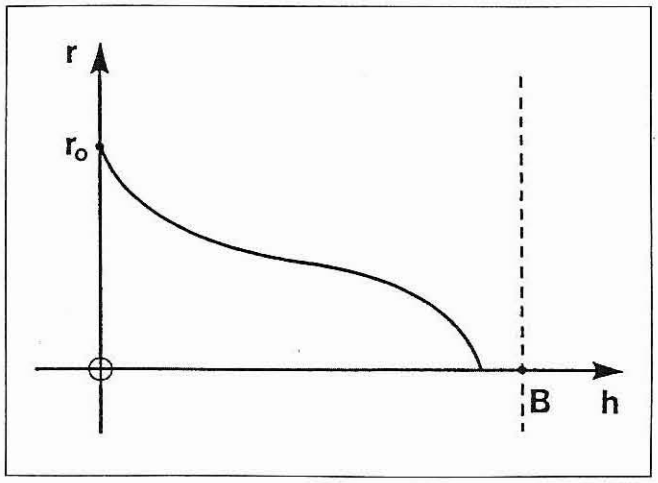

Fig. 4.2. The same graph as in Figure 4.1, but rotated clockwise, showing new axes and restricted to the first quadrant.

Table 4.1. Fitting equation (4.8) to the 10 *Eucalyptus cloeziana* trees listed in Table 1.1.

Tree No.	DBH O.B	Total Height	α	β	B	Mean Square Error
116	18.0	21.64	136.290	0.669	173.628	0.021
121	20.6	21.34	13.374	0.789	43.799	0.076
127	15.5	19.81	12.400	0.633	42.346	0.017
128	13.2	18.59	297.614	0.560	185.194	0.089
138	13.7	17.98	8.000	0.774	33.671	0.031
139	13.2	18.29	164.729	0.591	149.428	0.022
142	17.5	19.81	7.500	0.758	32.667	0.041
147	11.9	13.10	283.700	0.452	113.842	0.110
149	18.0	21.03	37.305	0.649	71.522	0.043
152	18.0	20.73	6.656	0.820	31.363	0.030

then solving for r we obtain

$$r(h) = r_0 - \alpha \exp. \left\{\frac{1}{\beta} \ln \left[\ln \left(\frac{B}{B-h}\right)\right]\right\}, \tag{4.4}$$

which is our fourth model.

(We briefly point out a mathematical subtlety in (4.4). The function r is in fact undefined at h = 0, nevertheless its graph will appear to originate at the point $(0,r_0)$. This is because r has the *limit-value* r_0 as h tends to 0. Formally:

$$\lim_{h \to 0} r(h) = r_0.$$

We take this to be sufficient for the purpose of modelling stem forms. At any rate, (4.6) below could be used in place of (4.4), in which case r *is* defined at h = 0, and $r(0) = r_0$ as desired).

In this model, as in that of § 3, we suggest that B may be related to maximum possible height. With B and r_0 taken as known, the other parameters may be estimated by the same methods as is used for the Weibull growth curve. Equation (4.3), in fact, yields such a method. Let

$$\begin{aligned} Y &= \ln \left[\ln \left(\frac{B}{B-h}\right)\right] \\ X &= \ln (r_0 - r) \\ M &= \beta \\ C &= -\beta \ln \alpha \end{aligned} \tag{4.5}$$

then (4.3) appears in the form Y = MX + C. Use data points to plot X against Y, then fit a straight line through these points (e.g. by using least squares). This yields M and C, and then from (4.5) we obtain

$$\beta = M \text{ and } \alpha = e^{-C/\beta}.$$

It is possible to force the function (4.4) to pass precisely through a selected point. For example, if (4.4) is required to pass through (b, r_b), this may be effected by forcing the corresponding straight line Y = MX + C to pass through the point $\left(\ln (r_0 - r_b), \ln \left[\ln \left(\frac{B}{B-b}\right)\right]\right)$. Such a restriction on the straight line fitted through the (X, Y) points may of course have the effect that the overall fit of (4.4) to the original data is not the best possible with this method. This would be the price to pay for forcing r(h) through a selected point.

Another way of forcing (4.4) through, say, (b, r_b) would be to interpret the origin in Figure 4.1 not as the point $(0, r_0)$ but as the point (b, r_b). Instead of the equations (4.2) we then have

$$\begin{aligned} h' &= h - b \\ r' &= r_b - r \end{aligned} \tag{4.6}$$

which leads in the same way as before to

$$\beta \ln (r_b - r) - \beta \ln \alpha = \ln \left[\ln \left(\frac{B}{B-(h-b)}\right)\right] \tag{4.7}$$

and then to

$$r(h) = r_b - \alpha \exp \left\{\frac{1}{\beta} \ln \left[\ln \left(\frac{B}{B-(h-b)}\right)\right]\right\} \tag{4.8}$$

The equations corresponding to (4.5) are then

$$\begin{aligned} Y &= \ln \left[\ln \left(\frac{B}{B-(h-b)}\right)\right] \\ X &= \ln (r_b - r) \\ M &= \beta \\ C &= -\beta \ln \alpha \end{aligned} \tag{4.9}$$

An assessment of this model appears in Table 4.1. Note that (4.8) is undefined for $0 \leq h < b$, so that this model in effect ignores the stem profile beneath breast height. Measurements below breast height were therefore disregarded when calculating the mean square errors listed in Table 4.1. (Note further that in fact (4.8) is also undefined for h = b, but that the situation is entirely analogous to that which obtains for h = 0 in (4.4), and that the same comments concerning limits therefore apply.)

5. Conclusion

We briefly summarize here the main features of each of the four models presented in this article.

The first model, given by equation (2.8) is obtained from two classic decay functions by subtraction – simple enough, but not very elegant. The function has three parameters, two of which are shape parameters for the initial part and the terminal part respectively, and the third is intended to approximate the radius at the point of inflection. Given extra data points in the initial part and the terminal part, respectively, there are simple formulae giving initial values for estimating the shape parameters. The function does not pass precisely through total height (H;0), nor through radius at breast height $(b;r_b)$, and it cannot be forced to do so. Because of its simplicity, the square of this function is analytically integrable. If, therefore, we view the bole of a tree modelled by this function r_1 as being represented by the volume of revolution obtained by revolving r_1 around the horizontal axis, then

$$\text{volume} = \pi \int_0^H [r_1 (h)]^2 \, dh. \tag{5.1}$$

Thus, given the integral of $r_1(h)^2$, finding volume is a simple calculation.

The second model, given by equation (2.14), arises as the solution of a differential equation. Like the first model it has three parameters, two for shape and one for size. Again the shape parameters are easily initialized given extra data points. In this case, too, the square of the function is analytically integrable. In addition, and here the second model has the advantage, the function passes precisely through the standard measurement point $(b;r_b)$, though not precisely through (H;0).

The third model, given by equation (3.7), may be viewed either as arising from a differential equation (which in turn arises from seemingly reasonable assumptions), or as arising directly from the logistic function by a translation and reorientation of axes. The function has three parameters, one for shape and two for size. One of the size parameters does not have an obvious physical interpretation. The shape parameter is easily initialized from an extra data point. The function passes precisely through $(b;r_b)$. If (3.8) is accepted as giving the precise value of k, then the function passes precisely through (H,0) as well.

The fourth model, given by equation (4.8), is obtained directly from the Weibull growth function by translation and re-orientation. It has three parameters, one for shape, one for scale and one for size. It does not arise from a differential equation, and there is no simple initialization procedure from a single data point. The function passes precisely through $(b;r_b)$, but this involves ignoring the stem profile beneath breast height. The function does not pass precisely through (H,0).

For a simultaneous comparison of all four models we present in Table 5.1 a summary of the four previous tables (MSE = mean square error). For this purpose we count a function as providing a »good fit« of a particular tree if it has MSE less than 0.1. On the basis of this table it would seem that the second and the fourth models are the most successful. But the sample of the trees used here is too small to give a definite verdict.

The main point of this article has been to show that taper functions modelling stem profiles may be obtained by using known growth and decay functions. We see in this a methodological simplification of the search for taper functions. There may not be a single »correct« or even »best« taper function – what is best may vary from one context to another. In our approach one may choose any growth or decay function having the structural properties required, and modify it to serve as a taper function.

We conclude with the remark that using growth or decay functions for obtaining taper functions may also lead to further taper functions. To illustrate this point, note that there is a structural similarity between the last two models (both obtained from growth functions). The third model, according now to equation (3.3), may be rewritten as

$$r(h) = r_0 - \frac{1}{KT_1}\left[\ln\left(\frac{B}{B-h}\right) + \ln\left(\frac{h+T_0}{T_0}\right)\right]. \qquad (5.2)$$

And the fourth model, according to equation (4.4), may be rewritten in the form

$$r(h) = r_0 - \alpha\left[\ln\left(\frac{B}{B-h}\right)\right]^{1/\beta}. \qquad (5.3)$$

Comparison of these two equations, (5.2) and (5.3), then shows that both models are of the form

$$r(h) = r_0 - C.F\left[\ln\left(\frac{B}{B-h}\right)\right],$$

Table 5.1. Summary of previous tables.

	model 1	model 2	model 3	model 4
Arithmetic mean of MSE's	0.0725	0.0607	0.164	0.048
Number of MSE's < 0.1	8	8	0	9
Smallest MSE	0.029	0.023	0.103	0.017
Largest MSE	0.113	0.135	0.246	0.110

where C is some constant and F is some function. That is, in both cases a taper function arises as some function F of $\ln\left(\frac{B}{B-h}\right)$. In (5.2) F is a linear function, in (5.3) F is a power function. So the models are similar in form, and differ in content only insofar as they modify

$$\ln\left(\frac{B}{B-h}\right)$$

in different ways, where B is some upper limit on h. Investigating other such modifications may be a fruitful line of further research.

Literature

BINGING, G. S., 1984: Taper equations for second-growth mixed conifers on Northern California. For. Sci. **30** (4), 1103–17.

DEMAERSCHALK, J. P., A. KOZAK, 1977: The whole-bole system – a conditioned dual-equation system for precise prediction of tree profiles. Can. J. For. Res. **7**, 488–497.

MADSEN, J. S., 1982: Determination of Stem Profiles in *Picea abies*. Faculty of Forestry, Royal Veterinary and Agricultural University, Copenhagen.

ORMEROD, D. W., 1973: A simple bole method. For. Chron. **49**, 136–138.

PRODAN, M., 1965: Holzmeßlehre. J. D. Sauerländer.

REED, D. D., J. C. BYRNE, 1985: A simple, variable form volume estimation system. For. Chron. **61** (2), 87–90.

YANG, R. C., A. KOZAK, J. H. G. SMITH, 1978: The potential of Weibull-type functions as flexible growth curves. Can. J. For. Res. **8** (4), 424–431.

Date of receipt: February 13th, 1986.

The authors' addresses: C. Brink, Department of Mathematics, University of Stellenbosch, Stellenbosch 7600, Republic of South Africa. K. von Gadow, z. Zt. Lehrstuhl für Waldwachstumskunde an der Universität München, Amalienstraße 52, D-8000 München 40.